

A robust metallo-oxidase from the hyperthermophilic bacterium *Aquifex aeolicus*

André T. Fernandes¹, Cláudio M. Soares¹, Manuela M. Pereira¹, Robert Huber², Gregor Grass³ and Lígia O. Martins¹

¹ Instituto de Tecnologia Química e Biológica, Universidade Nova de Lisboa, Oeiras, Portugal

² Lehrstuhl für Mikrobiologie, Universität Regensburg, Germany

³ Institute für Biologie/Mikrobiologie, Marthin Luther Universität, Halle, Germany

Keywords

Aquifex aeolicus; copper and iron homeostasis; hyperthermophilic bacteria; metallo-oxidase; multicopper oxidases

Correspondence

L. O. Martins, Instituto de Tecnologia Química e Biológica, Universidade Nova de Lisboa, Avenida da República, 2781-901 Oeiras, Portugal
Fax: +351 214411277
Tel: +351 214469534
E-mail: lmartins@itqb.unl.pt
Website: <http://www.itqb.unl.pt/martins>

(Received 22 January 2007, revised 13 March 2007, accepted 22 March 2007)

doi:10.1111/j.1742-4658.2007.05803.x

The gene, *Aquifex aeolicus* AAC07157.1, encoding a multicopper oxidase (McoA) and localized in the genome as part of a putative copper-resistance determinant, has been cloned, over-expressed in *Escherichia coli* and the recombinant enzyme purified to homogeneity. The purified enzyme shows spectroscopic and biochemical characteristics typical of the well-characterized multicopper oxidase family of enzymes. McoA presents higher specificity (k_{cat}/K_m) for cuprous and ferrous ions than for aromatic substrates and is therefore designated as a metallo-oxidase. Addition of copper is required for maximal catalytic efficiency. A comparative model structure of McoA has been constructed and a striking structural feature is the presence of a methionine-rich region (residues 321–363), reminiscent of those found in copper homeostasis proteins. The kinetic properties of a mutant enzyme, McoA Δ P321-V363, deleted in the methionine-rich region, provide evidence for the key role of this region in the modulation of the catalytic mechanism. McoA has an optimal temperature of 75 °C and presents remarkable heat stability at 80 and 90 °C, with activity lasting for up to 9 and 5 h, respectively. McoA probably contributes to copper and iron homeostasis in *A. aeolicus*.

The multicopper oxidases (MCOs) constitute a family of enzymes that present broad substrate specificity, oxidizing numerous aromatic phenols and amines. The one-electron oxidation of these substrates occurs concomitantly with a four-electron reduction of molecular oxygen to water. The redox reactions catalyzed by these enzymes depend on the presence of three copper sites, designated Cu types, 1, 2 and 3; a mononuclear T1 copper centre that is the primary acceptor for electrons; and a trinuclear centre comprising one T2 and two T3 copper ions that is involved in dioxygen reduction to water [1,2].

The laccases constitute a large subfamily of MCOs and have been implicated in various biological activ-

ities related to lignolysis, pigment formation, detoxification and pathogenesis [3]. Laccases have a great potential in various biotechnological processes mainly owing to their high relative nonspecific oxidation capacity, the lack of a requirement for cofactors and the use of readily available oxygen as an electron acceptor. A few MCO members are able to oxidize lower valence metal ions, such as Cu⁺, Fe²⁺ and Mn²⁺, with high specificity. These are thus designated as metallo-oxidases [4], and prominent metallo-oxidases, such as human ceruloplasmin, yeast ferroxidase Fet3p and CueO from *Escherichia coli*, are known to be critically involved in metal homeostasis mechanisms. In aerobic metabolism, metals such as

Abbreviations

ABTS, 2,2'-azino-bis-(3-ethylbenzo-6-thiazolinesulfonic acid); IPTG, isopropyl thio- β -D-galactoside; MCO, multicopper oxidase; McoA, multicopper oxidase from *Aquifex aeolicus*; SGZ, syringaldazine.

iron and copper, although essential for life, readily participate in reactions that result in the production of highly reactive oxygen species [5].

The catalytic and stability characteristics of bacterial laccases at the molecular level are of considerable interest and, as a model system, the CotA-laccase from *Bacillus subtilis* has been extensively studied [6–10]. The main objectives of such studies are to dissect the catalytic mechanisms using protein engineering techniques and to design laccases that better match biotechnological applications. Herein, these studies are extended to hyperthermophilic laccase-like enzymes. Our understanding of the structure–function relationships for the extremophilic enzymes is still limited, but their use offers new opportunities for biocatalysis as a result of their superior stability [11]. In genome databases, very few thermo and hyperthermophile microorganisms were found to contain predicted MCOs. However, the *Aquifex aeolicus* genome revealed a 1784 bp ORF (accession no. AAC07157.1) [12], which on the basis of an amino acid sequence with a similarity of some 30% to the CotA-laccase from *B. subtilis* or to CueO from *E. coli*, was putatively assigned as a multicopper oxidase. *A. aeolicus* is a microaerophilic, hydrogen-oxidizing, chemolithoautotrophic bacterium that grows between 58 and 95 °C, and optimally at 89 °C, occupying the deepest branch of the bacterial

phylogenetic tree [13]. The present study reports the spectroscopic properties and biochemical characterization of the recombinant multicopper oxidase from *A. aeolicus* (McoA). It is shown that McoA is a hyperthermostable copper-activated metallo-oxidase, with features typical of the well-known MCOs. However, one aspect of McoA is the presence of a Met-rich segment that is absent in the ‘classic’ MCOs. A kinetic analysis of a mutant enzyme from which this segment was deleted, McoAΔP321–V363, indicates that this region occludes the substrate binding site. These results agree with the structural model proposed and further suggest its involvement in the catalytic mechanism of the enzyme. We show that the Met-rich region is involved in copper binding. Together with the observation that McoA appears to be encoded in a copper-resistance determinant, the cuprous and ferrous oxidation competence of McoA may have a role in the suppression of copper and iron cytotoxicity.

Results and Discussion

McoA resembles CotA and CueO

Sequence alignment of *A. aeolicus* McoA with CueO and CotA clearly indicates that McoA is a member of the multicopper family of enzymes (Fig. 1). The first

McoA	<u>MDRRKFIKTSLSFALGFSVGGLSLLSCGGGGTTGSSSSGQSGTLSKQSLNIPGYFLPPDQQRVSI</u> ITAKWTTLEVIPGKSTDMVVEIDNEYN....PVI	95
CueO	<u>MLRRDFLKYSVALGVSALPLWSRAAFAERPALPIPDLLTADASN</u>RMQLIVKAGQSTFAGKNATWGYNGNLLGPAV	78
CotAMTLEKFVDALPIPDILKPVQSSKEK.....TYEVTMEECTHQLHRDLPPTRLWGYNGLFPGPPTI	60
Consensus	m r r f k n p	
McoA	FLRKGQTFSADEFVNNSS.....GEDS.....I I H W H G F R A P W K S D G H P Y A V K D G E T Y S Y P D F T I I D R S G T Y F Y H P H P H G R T	166
CueO	QLHKGKSVTVDIHNQL.....AEDT.....T L H W H G L E I P G I V D G G P Q G I I P A G G T R . T V T F T P E Q R A A T C W I H P H K H G K T	148
CotA	EVKRNENVYKWMNNLPSHTFLPIDHTIHHSDSQHEPEVKTVVHLHGGVTPDSDGYPEAWFSKDFEQTPGYFKREVYHYFNQQRGAILWYHHDHAMAALT	160
Consensus	n d h h d g h h t	
McoA	GYQVYYGLAGMIIIEDEDEDNLKQALDLEYGVIDIPLIIQDKTFDSSGQLVYNP.....MGHMGFGWDTILVNLTPNYPMDVERKVIYRFRILN	254
CueO	GRQVAMGLAGLVLIED.DE.IRKLRLPKQWIGIDDPVPIIQDKRFSADGQIDYQLDIM.....TAAVGFWDGDTLLTNGAIYQHSAPKGLWRLRLLN	237
CotA	RLNVIAGLVGAYLIHDPKE...K.RLKLPSDEYDVPLLIIDRTINEDGSLFYPSAPENPSPSLNPSIVPAFCGETILVNGKVVWYVELEPRKYRFRVIN	256
Consensus	g i d k d i d t i l n r r i n	
McoA	GSNARPYRLALLRGNQRMRFVWIGVEGGLDTPKEVNEILVAPGERIDILVDFRDSVNDVIKLYN..... <u>HPHNI</u>	325
CueO	GCNARSLNIAASD.N..RPLYVIASDGGLLAEPVKVTEPLLMGERFEVFLVDSGKAFDLVTLVPSQMGMAIAPFDKPHVPMRIQPLRITASGTLPDPTL	334
CotA	ASNTRTYNLSLDNGG...DFIQIGSDGGLLPRSVKLNLSFSLAPAERYDIIIDFT.AYEGESIILANSAG.....	321
Consensus	n r i g g l l e r d s l	
McoA	<u>IGMGMIQMRMGMERGMGNGMNMMDMGADNSFEFV</u> MEFRVTKDSAYDKSIPQR...LSEVTPINTDGAQVQRITLGMRRMVFTINGETWEDGYANP	421
CueO	TTPALPSLEGLTVRNKLK <u>MDPRLDMGMQMLMKYGAQAMSGMDHDSMNAHMOGGNMCHG</u> EPMDHGNMMDHSGMNHGAMGNMNHGGKFDPHNANFINGQV	434
CotACGDVNPETDANIMQFRVTKPLAQKDESRRPKYLASYPVQH.....ERIQN.....IRTLKLAGTQDEYGRPVL	386
Consensus		
McoA	QDINN...PKVLFQONNGDVVIEEYVNNVTGMYPHMHIGFQFQVLER.....SL.....GPLRATDLGWKDTVIVAPMETVRIAIVDMSHYPN	500
CueO	FDMNK...PMFAAQKGRHERWVIVSGVG.DMMLHPPHIIHGTQFRILSE.....NG.....KAPAAHRTGWKDTVRVEG.GISEVLVKFDHDAP	511
CotA	LLNNKRWHDPVTEHPKVGTTETIWSIINPTRGTHTPIHLHLVSRVLRDRRPFDIARYQESGELSYTGPVAVPPPPSEKGGKDTIQAHAGEVLRIAATFG...P	483
Consensus	n h h h l g w k d t	
McoA	EHQIYLLHCHILEHHDEGMMVNYRVN....	526
CueO	KEHAYMAHCHLLEHEDTGMLGFTV....	536
CotA	YSGRYVWHCHILEHEDYDMMRPMIDITDPHK	513
Consensus	h c h h m m	

Fig. 1. Amino acid sequence alignment of the multicopper oxidase from *A. aeolicus* (McoA) with CotA laccase from *B. subtilis* and with the metallo-oxidase CueO from *E. coli*. The consensus sequence of the twin-arginine translocation system is underlined for CueO and McoA. The copper ligands are all conserved (grey boxes), indicating that McoA is a multicopper oxidase. The two large loops spanning Ser41 to Gly60 and Phe321 to Val363 that have no counterparts of similar size on the templates are double underlined. The consensus sequence McoA protein in the NCBI database, with the accession number NP-213770-1, was annotated as a putative periplasmic cell division protein from *A. aeolicus*.

38 amino acids residues encoded by the *mcoA* gene probably constitute a putative signal peptide for the twin-arginine translocation system that signals the protein for the periplasmic space in a folded state [14], as is the case for *E. coli* CueO [15]. Although there is, as yet, no experimental evidence for the role of this leader sequence, *A. aeolicus* does possess putative twin-arginine translocation genes and, in addition, the N terminus of McoA (MDRRKFIK) significantly matches the twin-arginine translocation-consensus motif, S/TRRXFLK (Fig. 1) [14]. Overall, most of the structure of the *A. aeolicus* McoA can be reasonably modelled using CotA from *B. subtilis* and CueO from *E. coli* as template structures, except for the two large loops spanning Ser41 to Gly60 and Phe321 to Val363; these loops have no counterparts in the template structures (Fig. 2). The sequence segment presenting the greatest problem is Phe321 to Val363, which is very large and close to the T1 copper active site. This may be particularly important in view of the possibility that this segment may control the active site access to substrates, a controlling factor for this enzyme's substrate specificity. Figure 2A shows a superposition of the 60 different structures obtained in the last cycle of the comparative modelling procedure, highlighting the

Phe321 to Val363 loop in red. Although the conformation of this 42-residue segment remains an open question requiring experimental structural characterization, it is noteworthy that it contains 10 glycine and 12 methionine residues, as follows: PHNLIGMGMIGMRMGMGMERGMGMGNMMDMGMDNSEFEV. The metallo-oxidase CueO, an essential component of the copper regulatory mechanism in *E. coli* under aerobic conditions [15], contains a similar methionine-rich region (14 Met and 6 Gly residues in a 42-amino acid segment) [17]. The crystal structure of CueO, with an exogenous copper bound, has been determined, identifying a fifth copper-binding site in the Met-rich region in a position to mediate electron transfer from substrates to the T1 copper centre [18]. Furthermore, Met-rich sequence motifs are found in a number of proteins involved in copper metabolism, such as PcoA and PcoC from *E. coli* [19], and numerous bacterial homologues, leading to the suggestion that such regions are involved in copper binding [4]. It is therefore likely that the Met-rich motif of McoA has a similar function. In Fig. 2B–D, the active site (T1 Cu) of CotA, CueO and McoA multicopper oxidases are shown, respectively. The molecular surface is marked in magenta in the zone of the most exposed

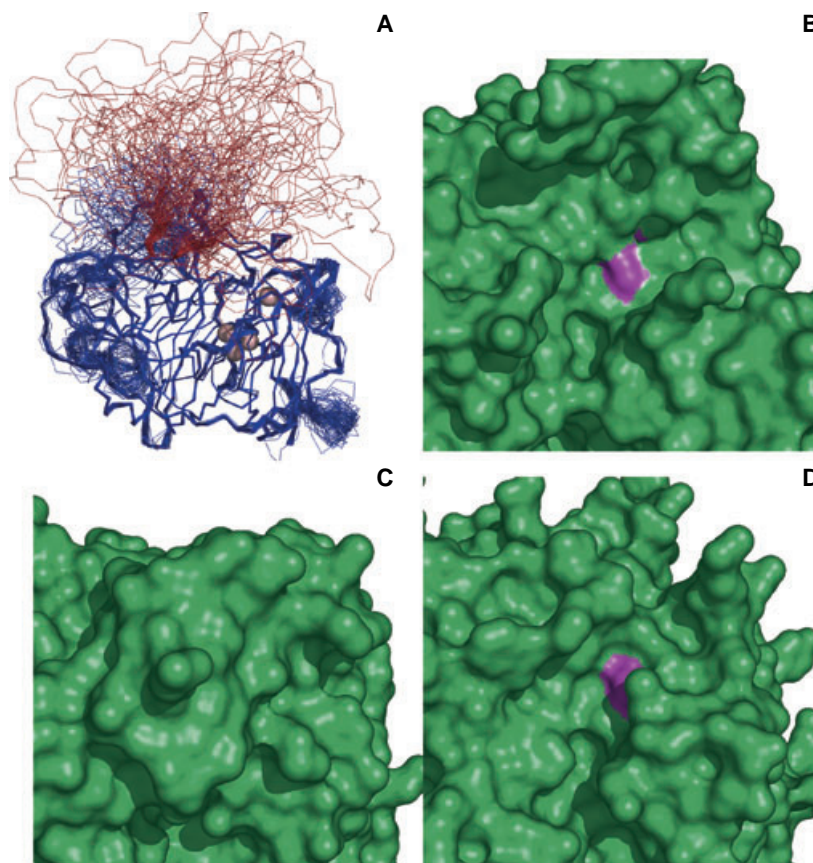


Fig. 2. (A) Overlay of the 60 different models obtained in the final cycle of the comparative modelling procedure for multicopper oxidase from *A. aeolicus* (McoA). The protein is represented by a thin ribbon and the copper atoms are represented by salmon-coloured spheres, with the T1 Cu ion separated from the three nuclear centres constituted by T2 and T3 Cu ions. The loop spanning residues Phe321 to Val363 is coloured in red, and the rest of the protein is coloured in blue. (B) Close-up of the active-site (T1 Cu centre) region of CotA, using a surface representation, highlighting (in magenta) the region of the most exposed histidine ligand of the copper, which is the residue that interacts with substrates. (C) Same as (B), but for CueO. (D) Same as (B), but for McoA. In this case, the Phe321 to Val363 loop was excluded from the model. This figure was prepared with PYMOL [16].

histidine residues that bind copper, highlighting, in this way, the active site accessibility. We can see that the three multicopper oxidases present considerable differences on the active site zone. The most exposed active site is that of CotA laccase, followed by McoA. Finally, the active site of CueO is buried (the histidine residue is not even exposed). Note that for this analysis, the Phe321 to Val363 segment was excluded in McoA, because there is no reliable structural information concerning its conformation. Therefore, this accessibility comparison must be handled with care, given that this segment may occlude the active site.

The *mcoA* gene is part of a putative copper-resistance determinant

A. aeolicus is a microaerophilic oxygen-respiring organism that thrives in geothermally and volcanically heated habitats, which are abundant in potentially toxic metals. In this regard it is interesting that the *mcoA* gene is located close to six genes, of which all but one codes for putative products with strong similarities to orthologues from characterized copper-resistance systems from *E. coli* (Fig. 3). All the genes are encoded on the *A. aeolicus* genome in the same direction of transcription. However, whether this determinant comprises a single operon or several independent transcriptional units has yet to be elucidated.

Overproduction and purification of recombinant wild-type McoA and McoA Δ P321-V363

The *mcoA* gene was cloned in pET-21a(+), resulting in pATF-1 that was transformed into *E. coli* Rosetta

(DE3) pLysS, yielding strain LOM409. SDS/PAGE analysis of crude extracts from LOM409 revealed that the addition of isopropyl thio- β -D-galactoside (IPTG) to the culture resulted in the accumulation of a major band of \approx 59 kDa in the insoluble fraction of cell lysates, most probably in the form of inclusion bodies (Fig. 4A), that was absent from extracts of uninduced LOM409. Attempts to produce the protein in the soluble form were unsuccessful. As a consequence, a protocol of unfolding and refolding was followed, as described in the Experimental procedures, and an enzyme solution with a blue colour (typical of blue multicopper oxidases) that exhibited enzymatic activity was successfully recovered. Dialysis and two chromatographic steps purified the protein to homogeneity (Fig. 4B). The protein was identified by MALDI-TOF-MS after tryptic digestion, with an identification score of 194 and sequence coverage of 46%. Gel filtration experiments gave a molecular mass value of 57.8 kDa, close to the theoretical value predicted for the monomer (59.5 kDa). The predicted isoelectric point of the enzyme was 5.33, whereas the measured isoelectric point of the purified enzyme was 4.12. To investigate the involvement of the Met-rich segment for McoA catalytic activity, a McoA Δ P321-V363 mutant protein was constructed that lacks this region. The expression of the mutant gene was comparable to that of wild-type McoA. The molecular mass of the mutant protein was \approx 4.5 kDa lower than the wild-type enzyme (Fig. 4B).

Spectroscopic characterization

McoA presents a typical UV-visible spectrum for MCO (Fig. 5A) with a band at \approx 600 nm that corresponds to

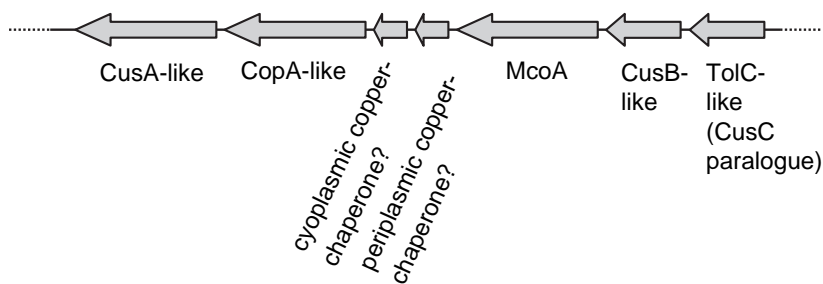
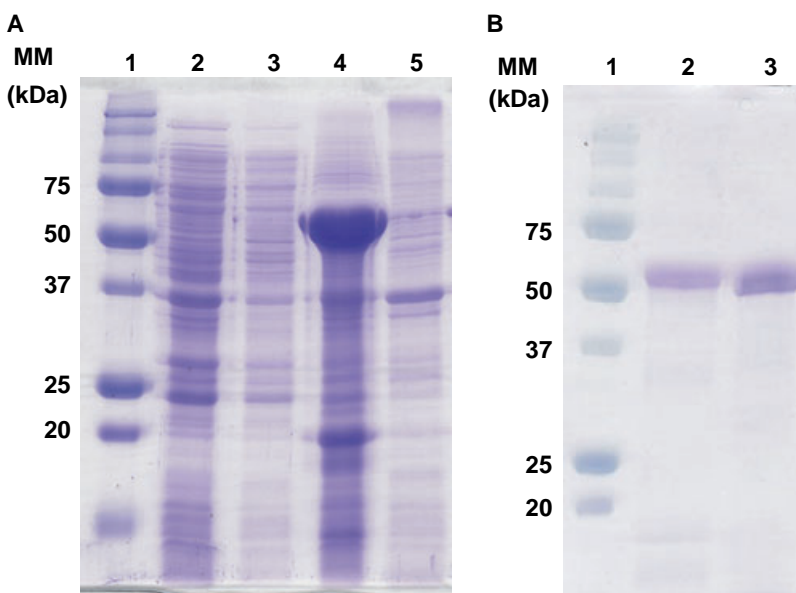


Fig. 3. The *mcoA* gene from *A. aeolicus* is part of a putative copper-resistance determinant. Five proteins with (and one without) similarity to known copper-detoxification systems are encoded in close vicinity to the *mcoA* gene, on the *A. aeolicus* genome. The CopA-like copper-efflux ATPase transports Cu(II) from the cytoplasm to the periplasm (34% identity to CopA from *Escherichia coli*), whereas the CusCBA-like tripartite transporter detoxifies periplasmic Cu(II) to the outside. The CusA-like pump protein of *A. aeolicus* shows 43% identity to CusA, and the CusB-like membrane fusion protein shows 23% identity to CusB from *E. coli*. In contrast, the putative outer membrane efflux duct protein of the *A. aeolicus* copper-resistance determinant shows higher similarity to TolC, a paralogue of CusC from *E. coli*. Additionally, two putative copper chaperones (accession nos AAC07166.1 and AAC07167.1) are present. The first bears similarity to the putative periplasmic copper chaperone, CopG protein, from several bacterial species. Each chaperone may be involved in the binding and delivery of copper to the respective cytoplasmic or periplasmic efflux pumps, thereby preventing the accumulation of 'free' redox-active Cu(II).

Fig. 4. (A) SDS/PAGE analysis of the multicopper oxidase from *A. aeolicus* (McoA) overproduction in *E. coli*. Lane 1, standard molecular mass markers; lanes 2 and 3, supernatant of a crude extract of IPTG-induced (lane 2) and noninduced (lane 3) *E. coli* LOM409 cells; lanes 4 and 5, insoluble fraction of a crude extract of IPTG-induced (lane 4) and noninduced (lane 5) *E. coli* LOM409 cells. (B) SDS/PAGE analysis of purified McoA and McoA Δ P321-V363. Lane 1, standard molecular mass marker; lane 2, purified wild-type McoA protein; and lane 3, purified McoA Δ P321-V363 mutant protein.



the Cu–Cys interaction at the T1 Cu centre and a shoulder at 330 nm, indicative of the presence of a hydroxyl group bridging the T3 copper ions [1]. A ratio of 2.5 mol of copper per mol of protein was found for recombinant McoA. This finding is not completely surprising as a lower copper content has already been reported for other recombinant MCOs, such as the bacterial CotA-laccase [6] and CueO from *E. coli* [20]. Indeed, copper incorporation in MCO has not been completely elucidated at the molecular level. The absorbance of mutant enzyme, McoA Δ P321-V363, at 610 nm, relative to 280 nm, showed 40% less intensity (data not shown) than the wild-type enzyme, suggesting that the mutation has slightly affected the copper incorporation into the T1 Cu site. The EPR spectrum of the McoA protein presents resonances characteristic of copper centres (Fig. 5B). Spectrum simulation revealed the presence of two components integrated in a ratio of 1 : 1. These components have EPR constants characteristics of T1 centres, with g -values of 2.044 and 2.222 and a hyperfine coupling $A_{\parallel} = 68 \times 10^{-4} \cdot \text{cm}^{-1}$, and of T2 centres, with g -values of 2.040, 2.055 and 2.260 and $A_{\parallel} = 169 \times 10^{-4} \cdot \text{cm}^{-1}$. T3 centres cannot be observed by EPR as a result of the antiferromagnetic coupling of the two constituent copper ions. The McoA mutant enzyme was not different from the wild-type regarding EPR spectroscopic characteristics (data not shown). The CD spectrum of McoA in the far-UV region reflected the typical secondary structure found in MCO, rich in β -sheets with a negative peak at 213–214 nm (Fig. 5C). Indeed, a secondary structure esti-

mate based on the CDSSTR method yielded values of 6% α -helical, 37% β -strand structure and more than 55% of turns and random coil structure [21]; these values were similar to those obtained by DSSP calculations based on the McoA model structure, namely 4% α -helical and 32% β -strand structure [22]. The CD spectrum of the mutant McoA Δ P321-V363 (data not shown) showed a small increase in α -helical and β -strand structure relative to the wild-type protein (from 6 to 8% and from 37 to 40%, respectively) and this correlates with the deletion of an unordered segment, as proposed in the model structure. This also clearly indicates that deletion of the Met-rich segment did not cause any gross disruption or reorganization of the structure. The redox potential was measured by following the decrease in absorbance at 610 nm, reflecting the reduction of the T1 copper of McoA. The normalized amplitude of the absorbance at 610 nm, and its dependence on the reduced potential, is shown in Fig. 6. The best fit was obtained using the Nernst equation, considering one electron transfer, with a redox potential of 535 mV. The mutant enzyme presents a redox potential of 494 mV (data not shown), only slightly lower than that of the wild-type enzyme. Redox potentials exhibited by MCO span a broad range of values, from 400 mV for plant laccases up to 790 mV for some fungal laccases [1].

McoA exhibits high metal oxidative activity

The steady-state kinetic parameters of purified *A. aeolicus* McoA were obtained for the metal ions Fe(II) and

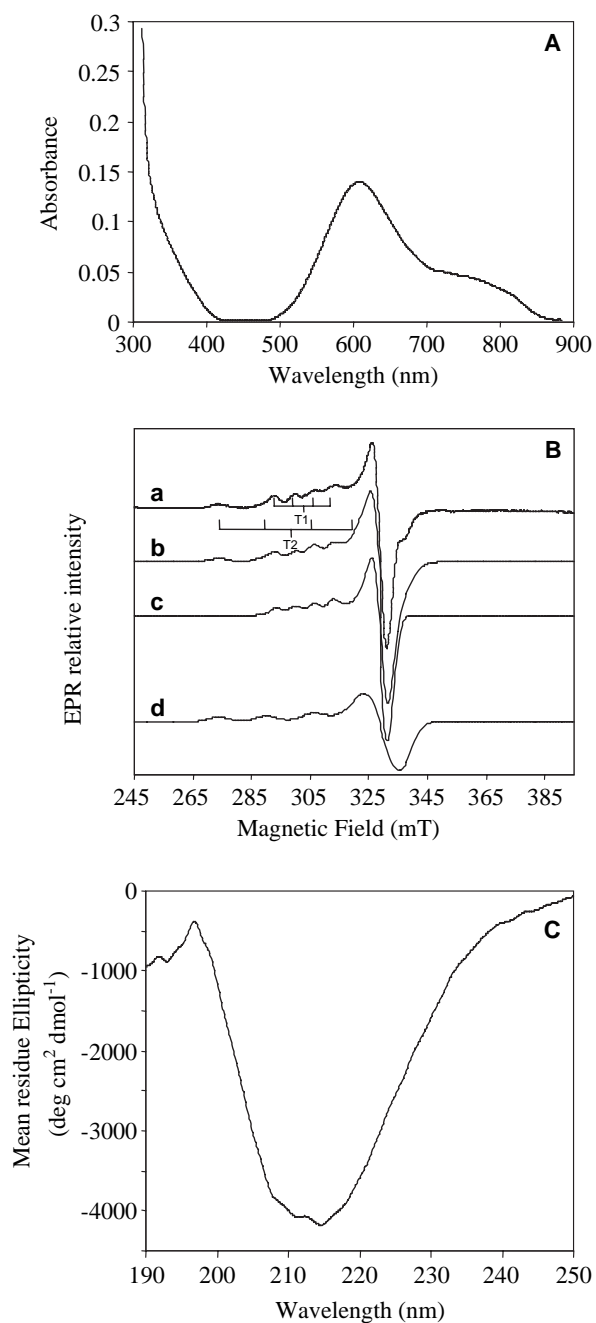


Fig. 5. Spectroscopic properties of recombinant purified multicopper oxidase from *A. aeolicus* (McoA). (A) UV-visible spectrum of McoA (70 μM in 20 mM Tris/HCl buffer, pH 7.6). (B) a, EPR spectrum of the purified McoA; b, simulation of the total spectrum; and c and d, deconvolution of the different components. In the simulation of the T1 center, g -values of 2.044, 2.044 and 2.222, and a hyperfine coupling constant $A_{\text{II}} = 68 \times 10^{-4} \text{cm}^{-1}$ were used, whereas for the T2 copper center, the g and A_{II} values used were 2.044, 2.055 and 2.260 and $169 \times 10^{-4} \text{cm}^{-1}$. Microwave frequency, 9.42 GHz; microwave power, 2.4 mW, modulation amplitude, 0.9 millitesla, temperature, 95 K. (C) CD spectrum in the far-UV region, reflecting a high β -sheet content.

Cu(I) and also for the substrates 2,2'-azinobis-(3-ethylbenzothiazoline-6-sulfonic acid) (ABTS) and syringaldazine (SGZ) in air-saturated solutions, at 40 °C (Table 1), as technical limitations prevented metal oxidation measurements at higher temperatures. The dependence of the enzymatic rates on substrate concentration followed Michaelis–Menten kinetics. The recombinant purified McoA exhibits higher enzyme efficiency (k_{cat}/K_m) for the oxidation of the metal ions compared with the phenolic and nonphenolic substrates, and thus McoA was designated a metallo-oxidase. Maximal effectiveness for the substrates tested was achieved upon addition of 100 μM CuCl_2 to the reaction mixture. This activation in the presence of cupric copper, resulted, for the metal substrates, from an increase in the k_{cat} values (indicating activation in the electron transfer kinetics) and for the larger substrates from a decrease in the K_m values (indicating steric changes in the substrate-binding pocket). Metal oxidase activities were also determined for purified human ceruloplasmin. With Fe(II) as substrate, apparent K_m and k_{cat} values of $28 \pm 2 \mu\text{M}$ and $8 \pm 2 \text{min}^{-1}$ were determined. For Cu(I) oxidation, the constants were $33 \pm 12 \mu\text{M}$ and $15 \pm 1 \text{min}^{-1}$. These kinetic values have the same order of magnitude as previous measurements for human ceruloplasmin [23]. The k_{cat}/K_m value of McoA for Cu(I) in the presence of exogenous copper is similar to that obtained for CueO from *E. coli* and two- to fourfold higher than for the yeast ferroxidase Fet3p and human ceruloplasmin [23,24]. McoA ferroxidase efficiency is threefold higher than for CueO or human ceruloplasmin and twofold lower than for yeast ferroxidase Fet3p [23,24]. All these data suggest that *A. aeolicus* McoA acts as a metallo-oxidase *in vivo*, functioning as a cytoprotector and shifting the Cu(II)/Cu(I) and Fe(III)/Fe(II) ratios in the periplasm of *A. aeolicus* towards the less toxic forms of copper and iron, Cu(II) and Fe(III). In fact, there is a growing indication of a link between periplasmic MCO and metal metabolism in bacteria that emerges from recent genetic, physiological and biochemical studies in strains such as *E. coli* [25], *Pseudomonas aeruginosa* [26], *Staphylococcus aureus* [27] and *Rhodobacter capsulatus* [28]. McoA has maximal activity at pH 4 and 7 for ABTS and SGZ, respectively (data not shown), consistent with those exhibited by a number of laccases [3]. The catalytic activity of McoA, for ABTS as the substrate, was found to increase from a value of 2.3 to 7.2 $\mu\text{mol}\cdot\text{min}^{-1}\cdot\text{mg protein}^{-1}$ at 40 °C and 75 °C, respectively (data not shown). The optimal temperature, 75 °C, is identical to that observed for the CotA laccase of *B. subtilis* [6], but lower than the 92 °C determined for the laccase of the thermophilic bacteria *Thermus thermophilus* [29].

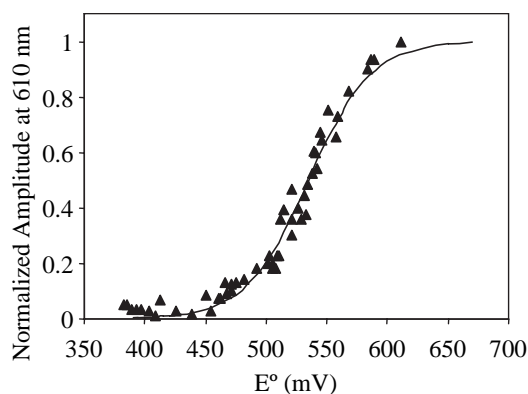


Fig. 6. Redox titration of the recombinant multicopper oxidase from *A. aeolicus* (McoA). The solid line shows the best fit of the experimental data obtained using the Nernst equation, considering one electron transfer, with a reduction potential of 535 mV.

The Met-rich region is involved in the catalytic mechanism of McoA

The deletion of the Met-rich segment of McoA resulted in a severe decrease in catalytic effectiveness for all the substrates tested (Table 1). The difference in the enzymatic efficiencies in the mutant McoA Δ P321-V363 compared with the wild-type enzyme relies essentially in the k_{cat} term, suggesting that the presence of the Met-rich motif and its conformational arrangement is a key factor of the catalytic mechanism. In addition, no enzyme activation upon addition of Cu(II) was observed in the mutant, showing that this segment probably modulates the participation of exogenous Cu(II) in the catalytic mechanism, presumably through binding, in analogy with what happens in CueO. In the structure of a CueO crystal soaked

in CuCl₂, a labile Cu(II) ion is bound by two aspartates, two methionines and a solvent molecule in the Met-segment near the T1 centre, providing a possible electronic matrix coupling pathway for electron transfer into this centre [18]. The mutagenesis of these four copper ligands resulted in the loss of oxidase activity and copper tolerance, confirming a regulatory role for this segment [18]. In the McoA mutant enzyme, decreased K_m values were found for the larger aromatic substrates, whereas these values remain basically unchanged for the smaller metal substrates when compared with the wild-type enzyme. This suggests that the Met-segment impairs the binding efficiency of larger substrates to the McoA substrate binding site as a result of steric effects. These data support a structure in which the Met-rich region masks the zone of the substrate-binding site near the T1 Cu centre, as observed in simulations of the McoA model structure. Interestingly, the K_m values for larger substrates in the mutant enzyme are similar to values obtained for the wild-type enzyme in the presence of copper. The presence of copper, and its probable binding to this region, might lead to a conformational change, causing an enlargement of the substrate-binding cavity. Clearly, more structural studies are required.

McoA is a hyperthermostable enzyme

The kinetic stability of an enzyme is relevant not only in the evaluation of its thermostability, but also in the study of the pathway that leads to the formation of irreversible inactivated states of the enzyme. McoA activity decay can be fitted only through a sum of two exponentials (Fig. 7A). This is clearly shown in a

Table 1. Kinetic parameters for oxidation of the metal ions Cu(I), Fe(II) and the typical laccase substrates, 2,2'-azinobis-(3-ethylbenzo-6-thiazolinesulfonic acid) (ABTS; a nonphenolic compound) and syringaldazine (SGZ; a phenolic compound) of the recombinant purified wild-type multicopper oxidase from *Aquifex aeolicus* (McoA) and its mutant variant, McoA Δ P321-V363, at 40 °C.

	Substrates	K_m (μM)	K_m (μM) + Cu(II) ^a	k_{cat} (min^{-1})	k_{cat} (min^{-1}) + Cu(II) ^a	k_{cat}/K_m ($\text{min}^{-1}\cdot\mu\text{M}^{-1}$)	k_{cat}/K_m ($\text{min}^{-1}\cdot\mu\text{M}^{-1}$) + Cu(II) ^a
Wild type	Cu(I) ^b	41 ± 2	46 ± 3	66 ± 5	165 ± 6	1.6	3.6
	Fe(II) ^c	5 ± 1	7 ± 2	17 ± 0.3	38 ± 0.6	3.4	5.4
	ABTS ^d	128 ± 8	59 ± 9	124 ± 5	114 ± 4	1.0	1.9
	SGZ ^e	38 ± 5	20 ± 3	29 ± 4	33 ± 6	0.8	1.7
McoA Δ P321-V363	Cu(I) ^b	39 ± 2	36 ± 5	8 ± 1	8 ± 0.3	0.2	0.23
	Fe(II) ^c	5 ± 2	9 ± 2	0.3 ± 0.01	0.2 ± 0.01	0.06	0.02
	ABTS ^d	57 ± 14	58 ± 11	0.41 ± 0.04	0.23 ± 0.05	0.005	0.004
	SGZ ^e	10 ± 3	12 ± 1	0.21 ± 0.02	0.11 ± 0.01	0.021	0.010

Optimal activity in the presence of ^a 100 μM CuCl₂, ^b 100 mM acetate buffer, pH 3.5 and 5% acetonitrile (optimal stability for the substrate); ^c 100 mM Mes buffer, pH 5 (optimal stability for the substrate), ^d Britton–Robinson buffer, pH 4 (optimal pH), and ^e in Britton–Robinson buffer, pH 7 (optimal pH).

semilogarithmic plot with two time ranges defining different linear relationships (insert of Fig. 7A). A series-type mechanism is commonly used to describe deactivation pathways composed of two steps, and this approach was used in the characterization of the kinetic stability of McoA (see Scheme 1, Experimental procedures). The decay of McoA at 80 °C is characterized by a first deactivation step (k_1) that lasts for 60 min, resulting in an intermediate state with 50% of the initial activity (β_1). This intermediate deactivates slowly (a lifetime of 490 min) to the final state that presents no activity (β_2). The same pathway describes McoA decay at 90 °C, but the rate constants of the two steps are higher, as expected (lifetimes of 25 and 269 min for the first and second steps, respectively). By measuring the amount of soluble McoA at the different times of thermal incubation, it was possible to assign the first phase of the activity decay to an aggregation process (Fig. 7B). The amount of soluble McoA at 80 °C decays accordingly to a single-exponential, giving a linear relationship when plotted as a semilogarithmic graph (inset in Fig. 7B). A lifetime of 53 min for the soluble species was calculated, very similar to the value of 60 min calculated for the first-phase of the activity decay. Therefore, the 50% decay of initial activity was shown to be caused by an aggregation process followed by a slow first-order step, as observed previously in other enzymes [30]. The values obtained here indicate the extreme robustness of the McoA enzyme. However, the *T. thermophilus* laccase, with a half-life of 868 min at 80 °C, is the most thermostable MCO that has been reported to date [29].

Experimental procedures

Construction of an expression plasmid for the *mcoA* gene

The *mcoA* gene was amplified by PCR using chromosomal DNA of strain *A. aeolicus* VF5 [13] and primers *mcoA*-182D (5'-ACTAAAGGAGGTAACATATGGACAGGC-3') and *mcoA*-1816R (5'-GACTTAGAATTCTCAACATATTGCCA-3'). The 1710 bp-long PCR product was digested with *Nde*I and *Eco*RI and inserted between the respective restriction sites of plasmid pET-21a(+) (Novagen, Darmstadt, Germany) to yield pATF-1. Analysis of the *mcoA* gene revealed that it contains uncommon codons for *E. coli*, including 25 for arginines, tRNA^{Arg}(AGG/AGA/CGG/CGA), 18 for leucines, tRNA^{Leu}(CTC) and 22 for isoleucines, tRNA^{Ile}(ATA). Therefore, the host strain Rosetta (DE3) pLysS (Novagen), expressing rare tRNAs, was used. Introduction of pATF-1 into Rosetta *E. coli* created strain LOM409, in which the

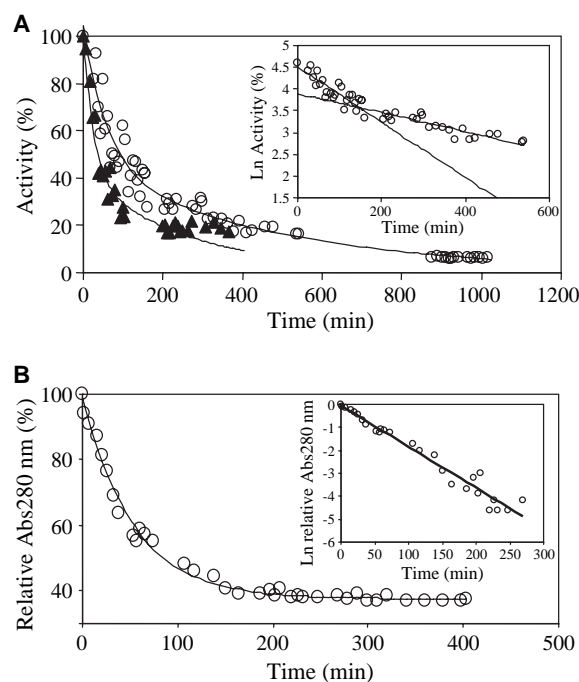


Fig. 7. (A) Kinetic stability of the multicopper oxidase from *A. aeolicus* (McoA). Stabilities at 80 °C (open circles) and 90 °C (black triangles) were fitted accurately through a sum of two exponentials (the solid line shows the fit) according to Scheme 1 shown in the Experimental procedures. The lifetime of the initial state, E , is 60 and 25 min at 80 and 90 °C, respectively. The intermediate state, E_1 , with 50% activity, has a lifetime of 490 and 269 min at 80 and 90 °C, respectively, before giving the final state, E_2 , with no activity. The inset shows clearly that the activity decay of McoA at both temperatures (data not shown for 90 °C) cannot be fitted by a single first-order process as the logarithm of activity does not display an inverse linear relationship with time. (B) Amount of McoA soluble at 80 °C, measured by the absorbance at 280 nm. The solid line shows a single-exponential fit with a rate constant of 0.019-min^{-1} (lifetime is 53 ± 2 min), an amplitude of 0.61 and an offset value of 0.38 (the offset value is the relative amount of McoA that remains soluble after completion and stabilization of the aggregates). The inset shows clearly that aggregation of McoA can be accurately fitted by a single exponential as proved by the inverse linear relationship between the logarithm of the relative absorbance at 280 nm (after discounting the offset value) and time.

McoA protein was produced under the control of the *T7lac* promoter.

Construction of an expression plasmid for *mcoA* not coding for a Met-rich segment

Phosphorylated primers, *mcoA*-del322r (5'-GAAGTTGTAAAGCTTTATTACGTCATTTAC-3') and *mcoA*-del362d (5'-GTTATGGAGTTCAGGGTTACAAAGG-3') were used to amplify around plasmid pATF-1, excluding an internal

fragment of *mcoA*. The PCR product was incubated with *DpnI*, to digest template DNA, self-ligated and introduced into *E. coli* DH5 α by transformation. The resulting plasmid, pATF-9, containing *mcoA* with an in-frame deletion corresponding to codons 964–1087, was introduced into the Rosetta *E. coli*-created strain, LOM420, in which the McoA mutant protein, McoA Δ P321-V363 was produced under the control of the T7lac promoter.

Overproduction and purification of McoA and McoA Δ P321-V363

Strains LOM409 (wild-type McoA) and LOM420 (McoA Δ P321-V363) were grown in Luria–Bertani (LB) culture medium supplemented with ampicillin (100 $\mu\text{g}\cdot\text{mL}^{-1}$) and chloramphenicol (34 $\mu\text{g}\cdot\text{mL}^{-1}$) at 37 °C. Growth was followed until an attenuation (*D*) of 1 at 600 nm was reached, at which time 100 μM IPTG and 250 μM CuCl₂ were added to the culture medium. Incubation was continued for a further 4 h. Cells were harvested by centrifugation (8000 *g*, 15 min, 4 °C). The cell pellet was suspended in 20 mM Tris/HCl buffer, pH 7.6, containing DNase I (10 $\mu\text{g}\cdot\text{mL}^{-1}$ of extract), MgCl₂ (5 mM) and a mixture of protease inhibitors (CompleteTM mini-EDTA free protease inhibitor mixture tablets; Roche, Basel, Switzerland). Cells were disrupted in a French pressure cell (at 19 000 psi), followed by centrifugation (18 000 *g*, 60 min, 4 °C). Soluble protein was recovered from inclusion bodies, based on a previously described method [31]. In short, the inclusion bodies were washed with 20 mM Tris/HCl buffer, pH 7.6, containing 0.5% Triton X-100, and spun down by centrifugation (12 000 *g*, 5 min, 4 °C). Inclusion bodies were unfolded in 20 mM Tris/HCl, pH 7.6, containing 8 M urea, 2 mM reduced glutathione and 0.2 mM oxidized glutathione, in a volume of 9 mL·g⁻¹ of pellet (at a final protein concentration below 2.5 mg·mL⁻¹) for 1 h at room temperature. Refolding was performed by slowly adding 9 mL (for each ml of urea-protein solution) of working buffer containing 2 mM reduced glutathione, 0.2 mM oxidized glutathione and 50 μM CuCl₂, and subsequent incubation for 2–4 h at room temperature. Dialysis in a Diaflow (Amicon, Billerica, MA, USA) with a 30 kDa (molecular weight cut-off) membrane was performed to remove urea. Refolded protein was resuspended in 20 mM Tris/HCl, pH 7.6, centrifuged and the resulting soluble fraction was loaded onto an ion exchange Q-Sepharose column (bed volume 25 mL) equilibrated with Tris/HCl (20 mM, pH 7.6). Elution was carried out with a two-step linear NaCl gradient (0–0.5 and 0.5–1 M) in the same buffer. Fractions were collected and assayed for activity. Active fractions were pooled, concentrated by ultrafiltration and equilibrated to 20 mM Tris/HCl, pH 7.6. The resulting sample was applied on a Superdex 200 HR 10/30 column (Amersham Biosciences, Piscataway, NJ, USA) equilibrated with 20 mM Tris/HCl

buffer, pH 7.6, containing 0.2 M NaCl. Active fractions were pooled, concentrated and incubated for 30 min with five equivalents of CuCl₂ per mole of McoA. Excess copper was removed by passing the solutions through a Sephadex G-25 column (PD 10 columns; Amersham Biosciences). All purification steps were carried out at room temperature in an FPLC system (Åkta-FPLC; Amersham Biosciences).

UV/visible, EPR and CD spectra

The UV/visible absorption spectra were obtained at room temperature in 20 mM Tris/HCl buffer, pH 7.6, using a Nicolet Evolution 300 spectrophotometer from Thermo Industries (Waltham, MA, USA). EPR spectra were measured with a Bruker EMX spectrometer (Rheinstetten, Germany) equipped with an Oxford Instruments ESR-900 continuous-flow helium cryostat (Oxford, UK). The spectra, obtained under nonsaturating conditions (160 μM protein content), were theoretically simulated using the approach of Aasa & Vänngård [32]. CD spectra in the far-UV region were measured on a Jasco-720 spectropolarimeter (Tokyo, Japan) using a circular quartz cuvette with a 0.01-cm optical pathlength in the range of 190–250 nm. Protein content was 25 μM in highly pure water (Milli-Q, Billerica, MA, USA).

Enzyme activities

Cuprous oxidase activity was measured in terms of rate of oxygen consumption by using an oxygen electrode (Oxygraph; Hansatech, Cambridge UK) at 40 °C, following the method described by Singh *et al.* [24]. Stock solutions of [Cu(I)(MeCN)₄]PF₆ (Sigma-Aldrich, St Louis, MO, USA) were freshly prepared in argon-purged acetonitrile and subsequently diluted anaerobically by using gas-tight syringes. Reactions were initiated by adding the substrate to an air-saturated mixture containing enzyme, 100 mM acetate buffer, pH 3.5, and 5% acetonitrile. The buffer was chosen to provide the best stability for the substrate used, and all reactions were corrected for background autoxidation rates of Cu(I). The oxidation of ABTS, SGZ and ferrous ammonium sulphate were photometrically monitored at 40 °C, unless otherwise stated, on either a Nicolet Evolution 300 spectrophotometer from Thermo Industries or a Molecular Devices (Sunnyvale, CA, USA) Spectra Max340 microplate reader with a 96-well plate. Ferrous ammonium sulphate oxidation was monitored at 315 nm ($\epsilon = 2200 \text{ M}^{-1}\cdot\text{cm}^{-1}$) in 100 mM Mes buffer, pH 5. The oxidation of ABTS and SGZ was followed at 420 nm ($\epsilon = 36\,000 \text{ M}^{-1}\cdot\text{cm}^{-1}$) and 530 nm ($\epsilon = 65\,000 \text{ M}^{-1}\cdot\text{cm}^{-1}$), respectively. Oxidations were determined using Britton-Robinson buffer (100 mM phosphoric acid, 100 mM boric acid and 100 mM acetic acid mixture titrated to the desired pH with 0.5 M NaOH). The standard reaction mixtures contained 1 mM ABTS (pH 4)

or 0.1 mM SGZ (pH 7). The effect of pH on the enzyme activity was determined at 40 °C for ABTS and SGZ in Britton–Robinson buffer (pH 3–9). The optimal temperature for the activity was determined at temperatures ranging from 40 to 90 °C by measuring ABTS oxidation at pH 4. Kinetic parameters were determined using reaction mixtures containing Cu(I) (5–300 µM, pH 3.5), Fe(II) (5–100 µM, pH 5), ABTS (50–400 µM, pH 4) and SGZ (1–100 µM, pH 7). The kinetic constants K_m and k_{cat} were fitted directly to the Michaelis–Menten equation (OriginLab, Northampton, MA, USA). All enzymatic assays were performed at least in triplicate. The specific activity was expressed as µmol of substrate oxidized $\text{min}^{-1}\cdot\text{mg}^{-1}$ of protein. The protein concentration was measured by using the absorbance band at 280 nm ($\epsilon_{280} = 75\,875\text{ M}^{-1}\cdot\text{cm}^{-1}$) or the Bradford assay [33], using bovine serum albumin as standard.

Redox titrations

Redox titrations were performed at 25 °C, pH 7.6, under an argon atmosphere, and monitored by visible spectroscopy (300–900 nm) in a Shimadzu Multispec-1501 spectrophotometer (Kyoto, Japan). The reaction mixture contained 25–50 µM enzyme in 20 mM Tris/HCl buffer, pH 7.6, and the following mediators each in a 10 µM final concentration (reduction potential between brackets); p-benzoquinone [+240 mV], dimethyl-p-phenylenediamine [+344 mV], potassium ferrocyanide [+436 mV] monocarboxylic acid ferrocene [+530 mV], 1,1'-dicarboxylic acid ferrocene [+644 mV] and Fe(II/III)-Tris-(1,10-phenantroline) [+1070 mV]. Potassium hexachloroiridate(IV) was used as the oxidant and sodium dithionite as the reductant. The redox potential measurements were performed with a combined silver/silver chloride electrode, calibrated with a quinhydrone-saturated solution at pH 7.0. The redox potentials are quoted against the standard hydrogen electrode.

Kinetic stability

Kinetic thermostability was determined at 80 or 90 °C by incubating an enzyme solution in 20 mM Tris/HCl buffer, pH 7.6. At appropriate time-points samples were withdrawn, cooled and immediately examined for residual activity following the oxidation of ABTS. The activity decay was fitted according to a second-order exponential model. This assumes an initial deactivation first-order step that leads to an intermediate state (E_1) displaying a fraction of the initial activity; β_1 is the ratio of activities between E_1 and the initial state, E . The state E_1 deactivates also according to a first-order step to give state E_2 with no activity in the case of McoA; β_2 is the ratio of activities between E_2 and the initial state. This deactivation model, previously used to describe the time-dependence deactivation of several other enzymes [34], was used as

McoA does not obey a more common first-order, single-step deactivation mechanism. The following scheme describes the two-step series model:



Considering that at time zero all the protein shares the conformation E and that the residual activity is determined by the activity of each conformational state weighted by its content, Eqn (1) was obtained and used to fit the time-dependence of residual activity [34] (where $f.act$ is fraction of activity, and t is time):

$$f.act = \left(1 + \frac{\beta_1 k_1}{k_2 - k_1} - \frac{\beta_2 k_2}{k_2 - k_1}\right) e^{-k_1 t} - \left(\frac{\beta_1 k_1}{k_2 - k_1} - \frac{\beta_2 k_2}{k_2 - k_1}\right) e^{-k_2 t} + \beta_2 \quad (1)$$

Structure of McoA by comparative modelling techniques

The structure of the *A. aeolicus* McoA was derived on the basis of the two bacterial MCOs present in the PDB – CotA from *B. subtilis* [7] (PDB code: 1GSK) and CueO from *E. coli* [17] (PDB code: 1KV7) – because these present considerably higher sequence identity (32.4% and 32.7%, respectively) than the eukaryotic multicopper oxidases with known structure. The program MODELLER [35], version 6.1, was used for deriving the structure. The alignment was optimized through several modelling cycles until a good quality model for the unknown structure was achieved. The quality was assessed by considering the restraint violations reported by MODELLER and a Ramachandran analysis performed by the program PROCHECK [36]. The final model (one of 60 structures with the lowest value of the MODELLER objective function) has 90.6% of the residues in the most favored regions, 8.3% in the additional allowed regions, 1.1% in the generously allowed regions and no residues in the disallowed regions. Two large loops of the McoA could not be modelled on the basis of the two known structures. The two loops span Ser41 to Gly60 and Phe321 to Val363. The latter is particularly long and presents considerable problems in the comparative modelling procedure. A decision was taken to model these two loops solely on the basis of stereochemical restraints and the general statistical preferences implemented in MODELLER.

Other methods

McoA peptides after tryptic digestion were analysed by MALDI-TOF-MS using a mass spectrophotometer Voyager STR (Applied Biosystems). Protein identification was performed using the peptide mass fingerprint as a query for the MASCOT-PMF software using the Swiss-Prot database. The molecular mass of the protein was determined on a gel

filtration Superose 12 HR10/30 column (Amersham Biosciences) equilibrated with 20 mM Tris HCl, pH 7.6, containing 0.2 M NaCl. Ribonuclease (13.7 kDa), chymotrypsinogen A (25 kDa), ovalbumin (43 kDa), albumin (67 kDa) and aldolase (158 kDa) were used as standards. The copper content was determined through the trichloroacetic acid/bicinchoninic acid method of Brenner & Harris [37] and confirmed by atomic absorption spectroscopy (Instituto Superior Técnico, Universidade Técnica de Lisboa, Chemical Analysis Facility). The isoelectric point was evaluated using IEF gels on a Phast System (Amersham Biosciences), with broad isoelectric point standards, following the manufacturer's instructions.

Acknowledgements

We thank our colleagues Peter F. Lindley and Eduardo P. Melo for useful discussions, P. F. Lindley and Isabel Bento for the provision of the purified sample of human ceruloplasmin, João Carita for help with the cell growth in the 'Organic Fermentation Unit' and Ana Coelho for the mass spectrometry measurements. This work was supported by project grant POCL/BIO/57083/2004.

References

- Solomon EI, Sundaram UM & Machonkin TE (1996) Multicopper oxidases and oxygenases. *Chem Rev* **96**, 2563–2605.
- Lindley PF (2001) Multi-copper oxidases. In *Handbook on Metalloproteins* (Bertini I, Sigel A & Sigel H, eds), pp. 763–811. Marcel Dekker, Inc., New York, NY.
- Xu F (1999) Recent progress in laccase study: properties, enzymology, production and applications. In *The Encyclopedia of Bioprocess Technology: Fermentation Biocatalysis, and Bioseparation* (Flickinger M-C & Drew SW, eds), pp. 1545–1554. John Wiley & Sons, Inc., New York, NY.
- Stoj CS & Kosman DJ (2005) Copper proteins: oxidases. In *Encyclopedia of Inorganic Chemistry*, Vol. II, 2nd edn. (King RB, ed.), pp. 1134–1159. John Wiley & Sons, New York, NY.
- Chrichton RR & Pierre J-L (2001) Old iron, young copper: from Mars to Venus. *Biometals* **14**, 99–112.
- Martins LO, Soares CM, Pereira MM, Teixeira M, Jones GH & Henriques AO (2002) Molecular and biochemical characterization of a highly stable bacterial laccase that occurs as a structural component of the *Bacillus subtilis* endospore coat. *J Biol Chem* **277**, 18849–18859.
- Enguita FJ, Martins LO, Henriques AO & Carrondo MA (2003) Crystal structure of a bacterial endospore coat component. A laccase enhanced thermostability properties. *J Biol Chem* **278**, 19416–19425.
- Enguita FJ, Marçal D, Martins LO, Grenha R, Henriques AO, Lindley PF & Carrondo MA (2004) Substrate and dioxygen binding to the endospore coat laccase from *Bacillus subtilis*. *J Biol Chem* **279**, 23472–23476.
- Bento I, Martins LO, Gato GL, Carrondo MA & Lindley PF (2005) Dioxygen reduction by multicopper oxidases: a structural perspective. *Dalton Transactions* **21**, 3507–3513.
- Durão P, Bento I, Fernandes AT, Melo EP, Lindley PF & Martins LO (2006) Perturbations of the T1 copper site in the CotA-laccase from *Bacillus subtilis*: structural, biochemical, enzymatic and stability studies. *J Biol Inorg Chem* **11**, 514–526.
- Egora E & Antranikian G (2005) Industrial relevance of thermophilic archaea. *Curr Opin Microbiol* **8**, 649–655.
- Deckert G, Warren PV, Gaasterland T, Young WG, Lenox AL, Grahams DE, Overbeck R, Snead MA, Keller M, Aujay M *et al.* (1998) The complete genome of the hyperthermophilic bacterium *Aquifex aeolicus*. *Nature* **392**, 353–358.
- Eder W & Huber R (2002) New isolates physiological properties of the *Aquificales* and description of *Thermocrinis albus* sp. Nov. *Extremophiles* **6**, 309–318.
- Stanley NR, Palmer T & Berks BC (2000) The twin arginine consensus motif of Tat signal peptides is involved in Sec-independent protein targeting in *Escherichia coli*. *J Biol Chem* **275**, 11591–11596.
- Grass G & Rensing C (2001) CueO is a multi-copper oxidase that confers copper tolerance in *Escherichia coli*. *Biochem Biophys Res Commun* **286**, 902–908.
- Delano W (2003) *The Pymol Molecular Graphics System*. Delano Scientific LLC, San Carlos, CA, USA.
- Roberts SA, Weichsel A, Grass G, Thakali K, Hazzard JT, Tollin G, Rensing C & Montfort WR (2002) Crystal structure and electron transfer kinetics of CueO, a multi-copper oxidase required for copper homeostasis in *Escherichia coli*. *Proc Natl Acad Sci USA* **99**, 2766–2771.
- Roberts SA, Wildner GF, Grass G, Weichsel A, Ambrus A, Rensing C & Montfort WR (2003) A labile regulatory copper ion lies near the T1 copper site in the multicopper oxidase CueO. *J Biol Chem* **278**, 31958–31963.
- Huffman DL, Huyett J, Outten FW, Doan PE, Finney LA, Hoffman BM & O'Halloran TV (2002) Spectroscopy of Cu (II)-PcoC and the multicopper oxidase function of PcoA, two essential components of *Escherichia coli* pco copper resistance operon. *Biochemistry* **41**, 10046–10055.
- Galli I, Musci G & di Patti MCB (2004) Sequential reconstitution of copper sites in the multicopper oxidase CueO. *J Biol Inorg Chem* **9**, 90–95.
- Sreerama N, Venyaminov SY & Woody RW (1999) Estimation of the number of alpha-helical and beta-strand segments in proteins using circular dichroism spectroscopy. *Protein Sci* **8**, 370–380.

- 22 Kabsch W & Sander C (1983) Dictionary of protein secondary structure: pattern recognition of hydrogen bonded and geometrical features. *Biopolymers* **22**, 2577–2637.
- 23 Stoj C & Kosman DJ (2003) Cuprous oxidase activity of yeast Fet3p and human ceruloplasmin: implication to function. *FEBS Lett* **554**, 422–426.
- 24 Singh SK, Grass G, Rensing C & Montfort WR (2004) Cuprous oxidase activity of CueO from *Escherichia coli*. *J Bacteriol* **186**, 7815–7817.
- 25 Grass G, Thakali K, Klebba PE, Thieme D, Müller A, Wildner GF & Rensing C (2004) Linkage between catecholate siderophores and the multicopper oxidase CueO in *Escherichia coli*. *J Bacteriol* **186**, 5826–5833.
- 26 Huston WM, Jennings MP & McEwan AE (2002) The multicopper oxidase of *Pseudomonas aeruginosa* is a ferroxidase with a central role in iron acquisition. *Mol Microbiol* **45**, 1741–1750.
- 27 Sitthisak S, Howieson K, Amezola C & Jayaswal RK (2005) Characterization of a multicopper oxidase gene from *Staphylococcus aureus*. *Appl Environ Microbiol* **71**, 650–663.
- 28 Wiethaus J, Wildner GF & Masepohl B (2006) The multicopper oxidase CutO confers copper tolerance to *Rhodobacter capsulatus*. *FEMS Microbiol Lett* **256**, 67–74.
- 29 Miyazaki K (2005) A hyperthermophilic laccase from *Thermus thermophilus*. *Extremophiles* **9**, 415–425.
- 30 Baptista RP, Chen LY, Paixão A, Cabral JMS & Melo EP (2003) A novel pathway to enzyme deactivation: the cutinase model. *Biotechnol Bioeng* **82**, 851–857.
- 31 Bollag DM, Rozycki MD & Edelman ST (1996) *Protein Methods*, 2nd edn. Wiley-Liss. John Wiley & Sons, New-York, Chichester, Brisbane, Toronto, Singapore.
- 32 Aasa R & Vängård VT (1975) EPR signal intensity and powder shapes: a reexamination. *J Magn Reson* **19**, 308–315.
- 33 Bradford MM (1976) A rapid and sensitive method for the quantification of microgram quantities of protein utilizing the principle of protein-dye binding. *Anal Biochem* **72**, 248–254.
- 34 Henley JP & Sadana A (1985) Characterization of enzyme deactivation using a series type mechanism. *Enzyme Microb Technol* **7**, 50–60.
- 35 Sali A & Blundell TL (1993) Comparative protein modelling by satisfaction of special restraints. *J Mol Biol* **234**, 779–815.
- 36 Laskowski A, MacArthur M, Moss D & Thornton J (1993) PROCHECK: a program to check the stereochemical quality of protein structures. *J Appl Cryst* **26**, 283–291.
- 37 Brenner AJ & Harris ED (1995) A quantitative test for copper using bicinchoninic acid. *Anal Biochem* **226**, 80–84.